Molecular Therapy
Nucleic Acids
Brief Report

Simple improvements in vector design afford substantial gains in AAV delivery of aggregation-slowing Aβ variants

Ella Borgenheimer,[1] Cameron Trueblood,[1] Bryan L. Nguyen,[2] William R. Lagor,[2] and Joanna L. Jankowsky[1,3]

[1]Department of Neuroscience, Baylor College of Medicine, Houston, TX 77030, USA; [2]Department of Integrative Physiology, Baylor College of Medicine, Houston, TX 77030, USA; [3]Departments of Neurology, Neurosurgery, and Molecular and Cellular Biology, Huffington Center on Aging, Baylor College of Medicine, Houston, TX 77030, USA

Adeno-associated virus (AAV) gene therapy for neurological disease has gained traction due to stunning advances in capsid evolution for CNS targeting. With AAV brain delivery now in focus, conventional improvements in viral expression vectors offer a complementary route for optimizing gene delivery. We previously introduced a novel AAV gene therapy to slow amyloid aggregation in the brain based on neuronal release of an Aβ sequence variant that inhibited fibrilization of wild-type Aβ. Here we explore three coding elements of the virally delivered DNA plasmid in an effort to maximize the production of therapeutic peptide in the brain. We demonstrate that simply replacing the Gaussia luciferase signal peptide with the mouse immunoglobulin heavy chain signal peptide increased release of variant Aβ by ∼5-fold. Sequence modifications within the expressed minigene further increased peptide release by promoting γ-secretase cleavage. Addition of a cytosolic fusion tag compatible with γ-secretase interaction allowed viral transduction to be tracked by immunostaining, independent from the variant Aβ peptide. Collectively these construct modifications increased neuronal production of therapeutic peptide by 10-fold upon intracranial AAV injection of neonatal mice. These findings demonstrate that modest changes in expression vector design can yield substantial gains in AAV efficiency for therapeutic applications.

INTRODUCTION

Recent advances in capsid evolution have transformed the potential for adeno-associated virus (AAV) gene therapy in the adult brain. Newly created serotypes now make it possible to deliver DNA throughout the CNS from a single, peripheral injection.[1] These breakthroughs in viral delivery have perhaps overshadowed more straightforward improvements in plasmid design to optimize expression of therapeutic payloads for improved efficacy. Here we examine three elements of the packaged AAV genome that we created to slow Aβ aggregation in Alzheimer's disease.

Alzheimer's disease is characterized by the pathological aggregation of amyloid β peptide (Aβ) into extracellular plaques and microtubule-associated tau protein (MAPT) into intraneuronal neurofibrillary tangles.[2,3] Extensive biochemical characterization has identified multiple sequence variants in each protein that can slow fibrilization of the wild-type monomer into neurotoxic aggregates; however, delivering these modified peptides into the brain has proven problematic.[4–6] In a recent study, we addressed this gap by vectorizing a small fragment of the amyloid precursor protein (APP) encoding a sequence variant of Aβ peptide, and showing that viral delivery of this peptide slowed amyloid formation in a mouse model of Alzheimer's disease.[7] Our work supported the potential of using virally delivered Aβ variants introduced directly into the brain before amyloid onset, but even small improvements to the vector would maximize our chance of success under the more challenging conditions of peripheral delivery after pathology has appeared.

Extracellular delivery of our Aβ variant into the brain depended on enzymatic processing of the APP fragment by endogenous γ-secretase within the plasma membrane.[7] Our original vector relied on the Gaussia luciferase signal peptide (GLSP) for membrane insertion. This signal peptide is derived from a marine copepod and although it is commonly used to express the Gaussia luciferase protein in mammalian cell lines,[8–10] it may be suboptimal for expression of other proteins such as ours.[11,12] Dozens of mammalian signal peptides and a growing number of synthetic versions have been identified, but finding the optimal match between signal sequence and expressed protein ultimately relies on empirical testing.[12–14] Two recent studies demonstrated efficient expression of the APP C-terminal fragment using the mouse immunoglobulin heavy chain V domain signal sequence (MoIgH).[15,16] Since our Aβ delivery vector was a shortened version of the APP C-terminal fragment, we took advantage of Xu and Yan's prior work to focus on the MoIgH sequence for comparison against GLSP.

We also examined whether altering the amino acids located near the γ-secretase site of our minigene could enhance proteolytic processing

Received 13 June 2024; accepted 22 August 2024;
https://doi.org/10.1016/j.omtn.2024.102314.

Correspondence: Joanna L. Jankowsky, Department of Neuroscience, Baylor College of Medicine, Houston, TX 77030, USA.
E-mail: jankowsk@bcm.edu

A

Construct name	Signal peptide	TM terminal amino acid	Cytosolic amino acids	Tag
KK	GLSP	L52	K53-K54	None
KK-V5	GLSP	L52	K53-K54	V5
KKK-V5	GLSP	L52	K53-K54-K55	V5
L52A-KKK-V5	GLSP	L52**A**	K53-K54-K55	V5
K53R-KK-V5	GLSP	L52	K53**R**-K54-K55	V5
L52A-K53R-KK-V5	GLSP	L52**A**	K53**R**-K54-K55	V5
KK-IRES-YFP	GLSP	L52	K53-K54	YFP
KKK-IRES-YFP	GLSP	L52	K53-K54-K55	YFP
KKK-P2A-YFP	GLSP	L52	K53-K54-K55	YFP
MoIgH-KKK-P2A-YFP	MoIgH	L52	K53-K54-K55	YFP
MoIgH-KKK-V5	MoIgH	L52	K53-K54-K55	V5

B

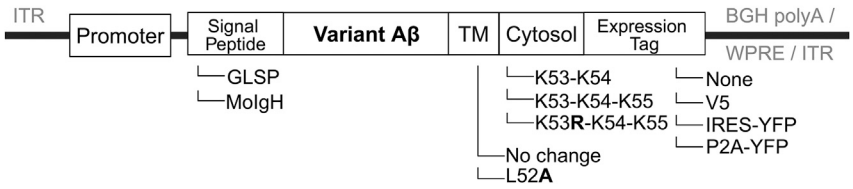

Figure 1. Three coding elements were tested to improve membrane delivery, enzymatic processing, and detection of the Aβ minigene

(A) Ten new vectors were created to test three design features: (1) Signal peptide from the mouse Ig heavy chain (MoIgH) was tested against the luciferase signal peptide from the copepod *Gaussia princeps* to determine if matching species of origin might improve membrane delivery. (2) Five juxtamembrane sequence variations were tested to optimize γ-secretase cleavage (composed of the final transmembrane (TM) residue plus two or three cytosolic residues, numbering starts from the Aβ N terminus as residue D1). (3) YFP and V5 cytosolic tags were tested for compatibility with Aβ release and to compare labeling fidelity. The original construct from Park et al. was designated as "KK" and used GLSP signal peptide with no cytosolic tag. (B) Diagram of the expression constructs indicating the location of each coding element. Plasmids were compared *in vitro* but designed for AAV packaging and brain delivery.

to increase extracellular release of our therapeutic peptide. Earlier studies discovered that an APP C-terminal fragment containing at least three intracellular lysines (KKK) increased γ-cleavage nearly 4-fold over a construct with just two lysines (KK).[16] This finding caught our attention as our initial APP minigene contained just two intracellular lysines and we wondered if we might improve cleavage efficiency—and increase Aβ release—by adding one more residue. The same research team identified two adjacent mutations at the membrane-cytosol boundary that further enhanced APP C-terminal processing (i.e., L52A and K53R[15,16]). We were keen to test whether these sequence modifications might improve γ-secretase processing of our APP minigene to further boost extracellular release of our Aβ variant peptide.

Finally, we wanted the new vector to provide some way of identifying viral expression that would not interfere with γ-secretase processing. Our past work used antibodies against the human Aβ sequence of our variant peptide to visualize viral spread in the mouse brain; however, this strategy identified both unprocessed APP minigene at the cell membrane and secreted Aβ peptide that diffused away from cells. We sought a cytosolic tag that would selectively identify viral expression. Based on the juxtamembrane charge requirement for γ-secretase cleavage determined by Xu et al.,[15] we ruled out flag, myc, and hemagglutinin tags which are all net negative sequences. Our final modification to the viral construct tested V5 against YFP as cellular tags for viral expression. We further examined whether an internal ribosome entry site (IRES) or self-cleaving P2A peptide would be the better route for YFP co-expression.

We show that these modest changes to the AAV expression vector provided a 10-fold increase in the amount of therapeutic peptide produced in the mouse brain.

RESULTS

Transfer plasmid optimization focused on three coding elements

Our original AAV vector for brain delivery of $A\beta^{F20P}$ variant peptide was based on a minigene encoding a small portion of full-length APP. Extracellular release of variant Aβ from the expressed APP fragment depended on two key design elements. First, the construct encoded an ectopic signal peptide for delivery to the plasma membrane. Second, the construct included the complete APP transmembrane domain plus two cytosolic lysines (KK) as a recognition motif for cleavage by endogenous γ-secretase that would release variant Aβ into the extracellular space where it could engage wild-type Aβ and prevent aggregation. Improving either of these elements should increase the amount of therapeutic peptide released from each transduced cell, and in theory should decrease the transduction threshold needed to impact amyloid accumulation. Our original construct carried no expression tag to see viral distribution. We could immunostain for the expressed human Aβ variant, but this did not formally distinguish secreted Aβ from the uncleaved membrane-bound protein in cells. Here we tested two well-used cytosolic tags to identify one that accurately identified transfected cells and was compatible with γ-secretase cleavage. In all, we tested 10 new AAV constructs against our original vector to identify the elements which maximized extracellular release of variant Aβ and reliably labeled cells carrying the construct (Figure 1).

Transient transfection provided comparison of secreted Aβ levels

We transfected 293T cells in triplicate with each of the 10 new transfer plasmids plus the original vector as a control. One set of cells was used for immunocytochemistry to determine how transfection efficiency compared across the constructs and

whether the expression tags faithfully reported cells that also produced human variant Aβ. We found no differences in qualitative transduction efficiency or fluorescence intensity of human Aβ immunostaining between cells transfected with the original Aβ F20P plasmid and those expressing the same plasmid with a V5 tag added to the cytosolic C terminus (Figure 2A, see KK vs. KK-V5). Across all of the V5-tagged constructs we tested, we found co-immunostaining for V5 showed good overlap with human Aβ expression, suggesting that the V5 fusion tag accurately reported localization and did not interfere with Aβ expression (Figure S1). We next compared the fidelity and efficiency of V5 as a cellular tag for plasmid localization against the two methods for YFP co-expression based on IRES and P2A. Of the three, P2A-YFP showed the highest transduction efficiency and good overlap with Aβ immunostaining (Figures 2B and S2). Unexpectedly, IRES-YFP did not co-label well with Aβ: many cells reported YFP without Aβ, and Aβ without YFP. Poor overlap between YFP and Aβ was found for both IRES-YFP constructs we tested, eliminating these constructs from final consideration.

A second set of cells was used to test protein expression in the cell lysate by western blot and Aβ secretion into the media by ELISA. All of the new constructs displayed an Aβ band at the expected size of ∼7–9 kD (Figure 2C). Relative to β-actin as a loading control, eight of the 10 new plasmids expressed at higher levels than the original vector (Figure 2D). Two notable exceptions were the P2A-YFP constructs: both had a strong Aβ band at ∼35 kD that co-stained for YFP, suggesting that much of the expressed protein had failed to self-cleave (Figure 2D). Given the poor fidelity of IRES-YFP constructs and failure of P2A-YFP cleavage, we chose the V5 tag instead of YFP for the final construct.

We next tested the concentration of secreted Aβ in the media. ELISA testing for Aβ40 revealed that the MoIgH signal peptide constructs secreted several-fold more Aβ into the media than constructs made with the original GLSP peptide (Figure 2E, see MoIgH-KKK-V5 vs. GLSP-KKK-V5). This experiment also demonstrated that the V5 tag did not interfere with γ-secretase cleavage required for Aβ release (Figure 2E, see KK vs. KK-V5). Finally, ELISA testing suggested that the double mutant L52A-K53R-KK-V5 produced slightly more secreted Aβ than the other V5 constructs relative to the amount of transfected protein detected on western blot (Figure 2E compared with Figure 2D).

We used the final well of transfected cells to ensure that Aβ secretion depended on γ-secretase processing to release mature peptide from the cell as intended. We treated cells with 1 nM of γ-secretase inhibitor LY411575 beginning 24 h after transfection and collected media 48 h later for Aβ ELISA. Aβ release from nine of the 11 constructs was reduced by >92%, with eight out of the 11 reduced by >96% (Figure 2E). The only constructs that were not inhibited by LY411575 were the two P2A-YFP plasmids, one of which was inhibited by <7% and the other was out of range, suggesting a similar lack of repression.

Taken together, these findings indicated that our final construct should contain the MoIgH signal peptide, a C terminus sequence ending in L52A-K53R-KK, and a V5 tag.

Neonatal brain transduction confirmed efficacy of the improved transfer plasmid

We next needed to test in mouse brain the three design elements we had shown to improve Aβ release in 293 cells. We cloned the original GLSP-Aβ^{F20P}-KK and the new MoIgH-Aβ^{F20P}-L52A-K53R-KK-V5 expression cassettes into an AAV transfer plasmid that contained the human synapsin promoter for expression in neurons (Figure 3A). Each plasmid was packaged into AAV8, and we injected each virus at two concentrations into the lateral ventricles of wild-type mouse pups shortly after birth (postnatal day 0, P0). AAV injection at this age allows widespread cortical transduction by viral diffusion through the immature ventricular lining.[17,18] This approach uses many-fold fewer viral particles for the same level of neuronal transduction compared with peripheral intravenous (i.v.) injection. Wild-type mice were chosen instead of APP transgenic models so that virally derived Aβ could be isolated from endogenous Aβ using human-specific Aβ detection kits and antibodies. Mice were harvested 3 weeks later and the brains hemisected for immunostaining and Aβ quantitation. Tissue immunostaining for Aβ revealed that the optimized construct expressed somewhat more strongly than the original, even though both viruses were injected at the same titers (Figure 3B). Co-immunostaining for V5 and Aβ showed good overlap between the two markers in mice treated with the optimized virus (Figure 3C). Cortical homogenates from the opposite hemisphere largely confirmed the visual impression from immunostaining. Aβ concentration was ∼10-fold higher in animals transduced with the new virus compared with the original construct (Figure 3D). Both Aβ40 and Aβ42 were increased without changing the overall ratio of 40:42.

DISCUSSION

We set out to determine if modest changes to our AAV delivery vector might increase release of therapeutic peptide from transduced cells. We also hoped to more accurately track viral expression using a fusion tag, without diminishing any gains in peptide release afforded from other changes to the sequence. Of the three modifications we investigated, the change from GLSP to MoIgH signal peptide had the greatest effect on peptide delivery. The APP has a native signal peptide that was not tested here,[19] but past work has shown that the native leader sequence is often not the optimal one for protein secretion.[11–13] Despite considerable commercial interest and *in silico* effort to create improved leader sequences, the efficiency of each signal peptide must be tested empirically and can vary with the expressed protein. Our experiments examined only two possibilities, but nevertheless increased peptide secretion 5- to 10-fold. This improvement should support better efficacy with less virus, or less efficient viral uptake, than our original construct. These are important considerations for viral gene therapy in humans where large quantities of virus are required for each patient, and transduction efficiency will be lower and more variable than in rodent models tested in the laboratory.

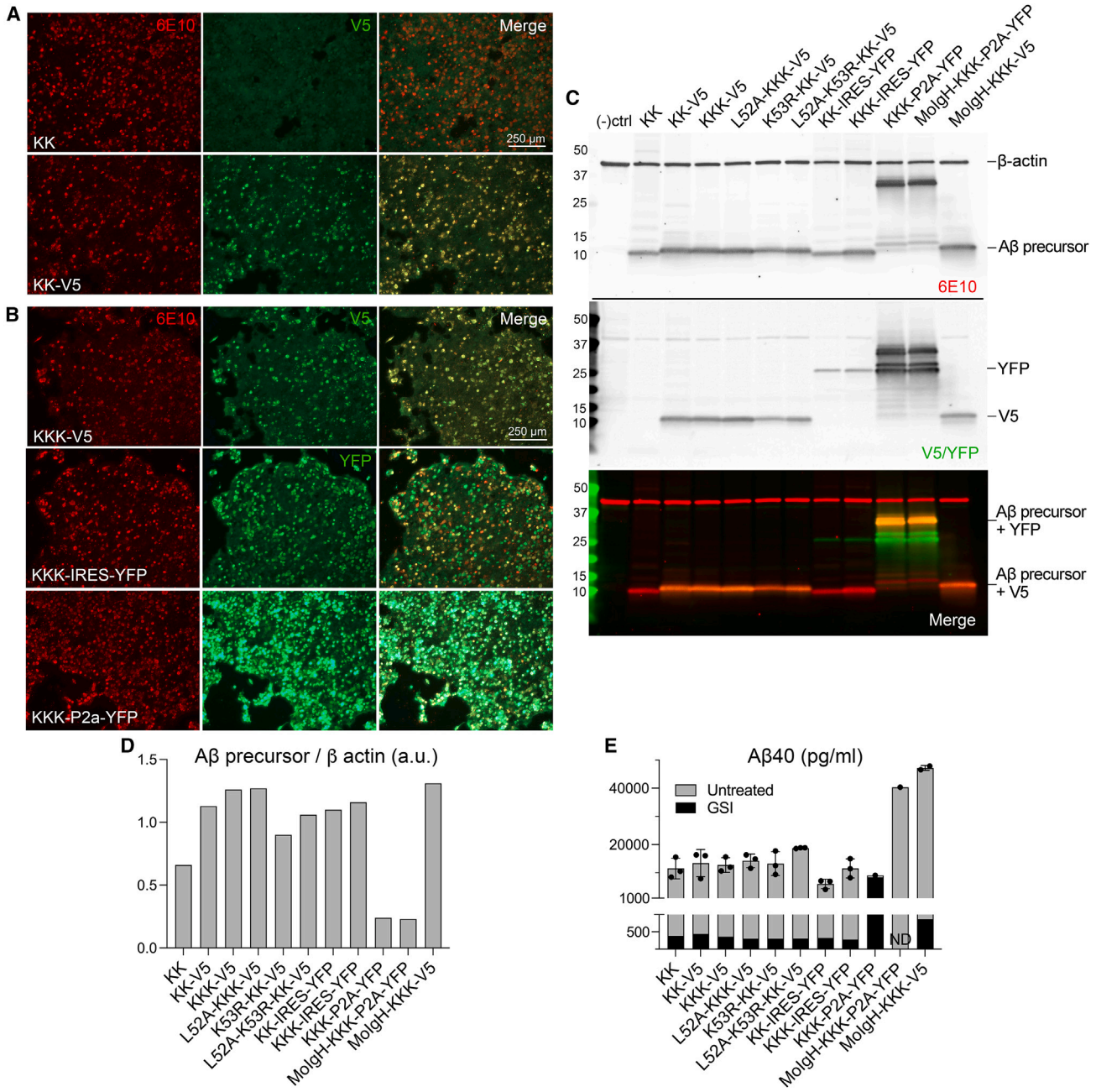

Figure 2. Transient expression in 293T cells was used to compare expression tags, transmembrane sequences, and signal peptides

(A) Transfected 293T cells were co-immunostained for human variant Aβ (6E10, red) and V5 (green). Addition of a V5 tag did not appreciably change the expression pattern of variant Aβ. (B) V5 was compared with YFP for cytosolic labeling in 293T cells. YFP was introduced using an IRES or a P2A peptide. Co-immunostaining for variant Aβ (6E10, red) and V5 (green) or YFP (green) revealed that the P2A construct had strongest fluorescence and that P2A-YFP and -V5 consistently co-labeled with Aβ, but IRES-YFP did not. (C) Western blotting of 293T cell lysates for Aβ (6E10, red) and V5 or YFP (green) confirmed that all constructs produce a band at the size expected for membrane-bound Aβ precursor and that all four YFP constructs produce a band at ~27 kD expected of free YFP, but that the two P2A-YFP constructs also produce an uncleaved Aβ+YFP fusion protein at ~37 kD. (D) The blot shown in (C) was quantified to determine the relative expression of Aβ minigene, normalized to β-actin. (E) Secreted Aβ was measured by ELISA in the media collected from transfected 293T cells. The MolgH signal peptide had greatest impact on Aβ release. Duplicate cultures were treated with γ-secretase inhibitor (GSI, black bars) and the media tested by Aβ ELISA. Aβ release was dependent on γ-secretase activity in all but the P2A-YFP constructs. Data are shown as mean ± SEM. ND, not determined - out of range.

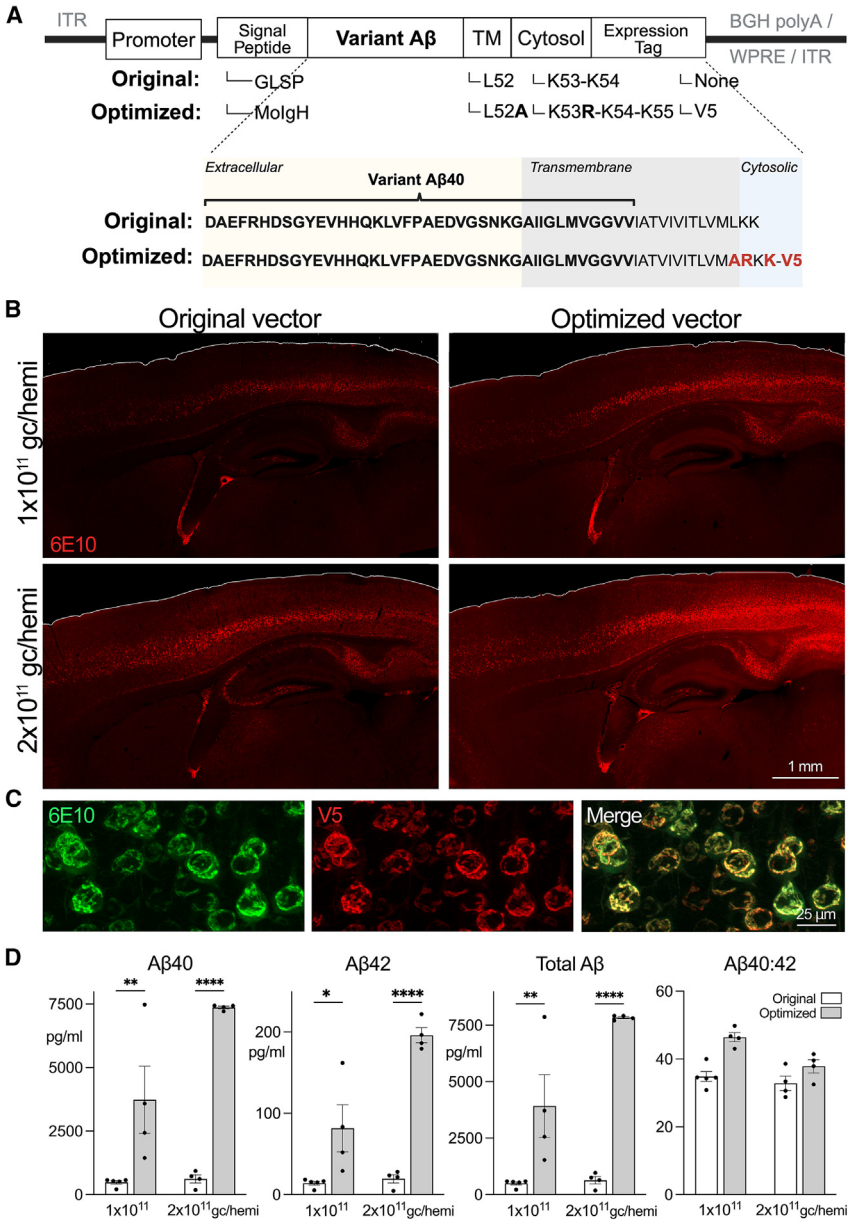

Figure 3. The optimized viral construct improved Aβ delivery in the mouse brain

(A) Vector diagram comparing our original and optimized AAV constructs for variant Aβ delivery. Inset below diagram illustrates the amino acid sequence of the APP minigenes and position relative to the membrane. (B–D) Original and optimized constructs were packaged into AAV8 and injected intracerebrovascularly (i.c.v.) into wild-type neonatal mice at a dose of 1×10^{11} genome copies (gc)/hemisphere (hemi) or 2×10^{11} gc/hemi. Mice were harvested 3 weeks later. (B) Immunostaining for human Aβ (6E10, red) demonstrates widespread viral expression of variant Aβ in a dose-dependent manner. Images show a portion of cortex and underlying hippocampus from sagittal brain sections. (C) Co-immunostaining for 6E10 (green) and V5 (red) in mice injected with the optimized construct shows good concordance between the two markers. Images show a magnified view of transduced neurons in frontal cortex. (D) Biochemical analysis of variant Aβ in cortical homogenates shows a significant increase of Aβ40, Aβ42, and total Aβ in the optimized construct without changing the Aβ40:42 ratio. ANOVA, $^{*}p \leq 0.05$, $^{**}p \leq 0.01$, $^{****}p \leq 0.0001$. Data are shown as mean ± SEM.

While we also found a small gain by modifying the transmembrane-cytosolic boundary sequence to improve γ-secretase cleavage, the other main outcome of our work was identifying a cytosolic tag that was compatible with secretase processing, well tolerated *in vivo*, and which accurately reported viral expression. We avoided several common expression tags such as flag, myc, and hemagglutinin, based on predicted incompatibility with γ-secretase due to negative charge.[15] We also ruled out two approaches for YFP co-expression. We found that the P2A-YFP cassette expressed strongly, but failed to self-cleave effectively, resulting in a large fusion protein that interfered with γ-secretase function. We tried a more traditional IRES-YFP approach, and while this produced an independent YFP protein, it did not accurately co-express with the Aβ variant. While the trailing cistron following an IRES (YFP) is frequently associated with lower expression levels than the upstream cistron (Aβ),[20] we also found cells that were YFP+ without Aβ. This outcome was unexpected but has been reported previously for some constructs carrying IRES-GFP, depending on the specific gene encoded in the first cistron.[21] Other groups have found variable co-expression between first and second cistrons, depending on the IRES used, the genes encoded, the cell type studied, and the relative position of each gene within the construct.[22–24] These results reiterate the value in empirically testing each vector component. By doing so we avoided potential pitfalls with YFP co-expression and simultaneously identified a much better signal peptide for our Aβ minigene.

MATERIALS AND METHODS

Materials and methods are provided in the online supplemental information.

DATA AND CODE AVAILABILITY

All the data related to this study are available within the paper or can be obtained from the corresponding author on request.

ACKNOWLEDGMENTS

We thank Emily Koller, Kyung-Won Park, Caleb Wood, and Jun Li for help with plasmid construction, the ORION core at MD Anderson Cancer Center for reading MSD V-PLEX plates, and Zoe Lai and Chelsea Zong for animal care. This work was funded by NIH RF1 AG069721-01A1 and -01A1S1, and Texas Alzheimer's Research and Care Consortium award 2020-02-11-II to J.L.J.

AUTHOR CONTRIBUTIONS

Conceptualization: J.L.J.; Formal analysis: C.T., E.B.; Funding acquisition: J.L.J.; Investigation: C.T., E.B., B.L.N.; Project management: J.L.J.; Resources: B.L.; Supervision: J.L.J.; Visualization: C.T., E.B., J.L.J.; Writing-original draft: J.L.J.; Writing-review and editing: all authors.

DECLARATION OF INTERESTS

The authors declare no competing interests.

C.T. is currently a paid employee of Eli Lilly and Co. but was not affiliated with this company or any for-profit entity at the time she contributed to this study.

J.L.J. is a co-inventor on pending patent application WO 202213346, Delivery of Abeta variants for aggregation inhibition.

SUPPLEMENTAL INFORMATION

Supplemental information can be found online at https://doi.org/10.1016/j.omtn.2024.102314.

REFERENCES

1. Challis, R.C., Ravindra Kumar, S., Chen, X., Goertsen, D., Coughlin, G.M., Hori, A.M., Chuapoco, M.R., Otis, T.S., Miles, T.F., and Gradinaru, V. (2022). Adeno-Associated Virus Toolkit to Target Diverse Brain Cells. Annu. Rev. Neurosci. *45*, 447–469.
2. Quan, M., Cao, S., Wang, Q., Wang, S., and Jia, J. (2023). Genetic Phenotypes of Alzheimer's Disease: Mechanisms and Potential Therapy. Phenomics *3*, 333–349.
3. Long, J.M., and Holtzman, D.M. (2019). Alzheimer Disease: An Update on Pathobiology and Treatment Strategies. Cell *179*, 312–339.
4. Lewis, A.L., and Richard, J. (2015). Challenges in the delivery of peptide drugs: an industry perspective. Ther. Deliv. *6*, 149–163.
5. Goyal, D., Shuaib, S., Mann, S., and Goyal, B. (2017). Rationally Designed Peptides and Peptidomimetics as Inhibitors of Amyloid-beta (Abeta) Aggregation: Potential Therapeutics of Alzheimer's Disease. ACS Comb. Sci. *19*, 55–80.
6. Ryan, P., Patel, B., Makwana, V., Jadhav, H.R., Kiefel, M., Davey, A., Reekie, T.A., Rudrawar, S., and Kassiou, M. (2018). Peptides, Peptidomimetics, and Carbohydrate-Peptide Conjugates as Amyloidogenic Aggregation Inhibitors for Alzheimer's Disease. ACS Chem. Neurosci. *9*, 1530–1551.
7. Park, K.W., Wood, C.A., Li, J., Taylor, B.C., Oh, S., Young, N.L., and Jankowsky, J.L. (2021). Gene therapy using Abeta variants for amyloid reduction. Mol. Ther. *29*, 2294–2307.
8. Tannous, B.A. (2009). Gaussia luciferase reporter assay for monitoring biological processes in culture and in vivo. Nat. Protoc. *4*, 582–591.
9. Tannous, B.A., Kim, D.E., Fernandez, J.L., Weissleder, R., and Breakefield, X.O. (2005). Codon-optimized Gaussia luciferase cDNA for mammalian gene expression in culture and in vivo. Mol. Ther. *11*, 435–443.
10. Knappskog, S., Ravneberg, H., Gjerdrum, C., Trösse, C., Stern, B., and Pryme, I.F. (2007). The level of synthesis and secretion of Gaussia princeps luciferase in transfected CHO cells is heavily dependent on the choice of signal peptide. J. Biotechnol. *128*, 705–715.
11. Chen, W., Zhao, X., Zhang, M., Yuan, Y., Ge, L., Tang, B., Xu, X., Cao, L., and Guo, H. (2016). High-efficiency secretory expression of human neutrophil gelatinase-associated lipocalin from mammalian cell lines with human serum albumin signal peptide. Protein Expr. Purif. *118*, 105–112.
12. O'Neill, P., Mistry, R.K., Brown, A.J., and James, D.C. (2023). Protein-Specific Signal Peptides for Mammalian Vector Engineering. ACS Synth. Biol. *12*, 2339–2352.
13. Gupta, K., Parasnis, M., Jain, R., and Dandekar, P. (2019). Vector-related stratagems for enhanced monoclonal antibody production in mammalian cells. Biotechnol. Adv. *37*, 107415.
14. Park, J.H., Lee, H.M., Jin, E.J., Lee, E.J., Kang, Y.J., Kim, S., Yoo, S.S., Lee, G.M., and Kim, Y.G. (2022). Development of an in vitro screening system for synthetic signal peptide in mammalian cell-based protein production. Appl. Microbiol. Biotechnol. *106*, 3571–3582.
15. Xu, T.H., Yan, Y., Kang, Y., Jiang, Y., Melcher, K., and Xu, H.E. (2016). Alzheimer's disease-associated mutations increase amyloid precursor protein resistance to gamma-secretase cleavage and the Abeta42/Abeta40 ratio. Cell Discov. *2*, 16026.
16. Yan, Y., Xu, T.H., Melcher, K., and Xu, H.E. (2017). Defining the minimum substrate and charge recognition model of gamma-secretase. Acta Pharmacol. Sin. *38*, 1412–1424.
17. Passini, M.A., and Wolfe, J.H. (2001). Widespread gene delivery and structure-specific patterns of expression in the brain after intraventricular injections of neonatal mice with an adeno-associated virus vector. J. Virol. *75*, 12382–12392.
18. Kim, J.Y., Ash, R.T., Ceballos-Diaz, C., Levites, Y., Golde, T.E., Smirnakis, S.M., and Jankowsky, J.L. (2013). Viral transduction of the neonatal brain delivers controllable genetic mosaicism for visualising and manipulating neuronal circuits in vivo. Eur. J. Neurosci. *37*, 1203–1220.
19. Selkoe, D.J. (2001). Alzheimer's disease: genes, proteins, and therapy. Physiol. Rev. *81*, 741–766.
20. Mizuguchi, H., Xu, Z., Ishii-Watabe, A., Uchida, E., and Hayakawa, T. (2000). IRES-dependent second gene expression is significantly lower than cap-dependent first gene expression in a bicistronic vector. Mol. Ther. *1*, 376–382.
21. Mansha, M., Wasim, M., Ploner, C., Hussain, A., Latif, A.A., Tariq, M., and Kofler, A. (2012). Problems encountered in bicistronic IRES-GFP expression vectors employed in functional analyses of GC-induced genes. Mol. Biol. Rep. *39*, 10227–10234.
22. Bochkov, Y.A., and Palmenberg, A.C. (2006). Translational efficiency of EMCV IRES in bicistronic vectors is dependent upon IRES sequence and gene location. Biotechniques *41*, 283–284. 286, 288 passim.
23. Sadikoglou, E., Daoutsali, E., Petridou, E., Grigoriou, M., and Skavdis, G. (2014). Comparative analysis of internal ribosomal entry sites as molecular tools for bicistronic expression. J. Biotechnol. *181*, 31–34.
24. Licursi, M., Christian, S.L., Pongnopparat, T., and Hirasawa, K. (2011). In vitro and in vivo comparison of viral and cellular internal ribosome entry sites for bicistronic vector expression. Gene Ther. *18*, 631–636.